Макрогетероциклы
http://mhc-isuct.ru

DOI: 10.6060/mhc267216g

2,6-Dimethylphenoxy Substituted Magnesium(II) Phthalocyanine and Boron(III) Subphthalocyanine: Synthesis, Photochemical Properties and Stability in Solutions

Elena A. Gorbunova,[a@] Karina A. Kisliak,[a] Alina S. Agranat,[a] Vyacheslav L. Baklagin,[b] Vladimir V. Bukhalin,[b] Igor G. Abramov,[b] and Tatiana V. Dubinina[a]

[a]*Department of Chemistry, Lomonosov Moscow State University, 119991 Moscow, Russian Federation*
[b]*Deparment of General Chemical Education, Yaroslavl State Technical University, 150023 Yaroslavl, Russia*
[@]*E-mail: lena.kuzmina94@gmail.com*

Boron(III) subphthalocyanine and magnesium(II) phthalocyanine bearing bulky 2,6-dimethylphenoxy groups were successfully prepared using template method. The influence of the macrocycle nature on the optical and photochemical properties, as well as stability in various solvents, was investigated. Target compounds demonstrated stability during 24 hours in THF, toluene and DMF. The subphthalocyanine complex was shown to be more efficient as a fluorophore (Φ_{Fl}=0.43), while the magnesium complex demonstrated higher singlet oxygen generation efficiency (Φ_{Δ}=0.42). The quantum yield of singlet oxygen of the obtained 2,6-dimethylphenoxy substituted magnesium phthalocyanine is higher than those of the well-known photosensitizer Photosens (Φ_{Δ}=0.19 in DMF).

Keywords: Phthalocyanine, subphthalocyanine, singlet oxygen, fluorescence, stability.

2,6-Диметилфеноксизамещенные фталоцианин магния(II) и субфталоцианин бора(III): синтез, фотохимические свойства и стабильность в растворах

Е. А. Горбунова,[a@] К. А. Кисляк,[a] А. С. Агранат,[a] В. Л. Баклагин,[b] В. В. Бухалин,[b] И. Г. Абрамов,[b] Т. В. Дубинина[a]

[a]*Химический факультет, Московский государственный университет имени М.В. Ломоносова, 119991 Москва, Российская Федерация*
[b]*Ярославский государственный технический университет, 150023 Ярославль, Российская Федерация*
[@]*E-mail: lena.kuzmina94@gmail.com*

Субфталоцианин бора(III) и фталоцианин магния(II), содержащие объёмные 2,6-диметилфеноксигруппы, получены с использованием темплатного метода. Исследовано влияние природы макроцикла на оптические и фотохимические свойства, а также стабильность в различных растворителях. Целевые соединения продемонстрировали стабильность в течение 24 часов в растворах тетрагидрофурана, толуола и диметилформамида. Комплекс субфталоцианина оказался более эффективным в качестве флуорофора (Φ_{Fl} = 0.43), в то время как комплекс магния продемонстрировал более высокую эффективность генерации синглетного кислорода (Φ_{Δ} = 0.42). Квантовый выход синглетного кислорода полученного 2,6-диметилфеноксизамещенного фталоцианина магния выше, чем у известного фотосенсибилизатора Фотосенс (Φ_{Δ} = 0.19 в ДМФА).

Ключевые слова: Фталоцианин, субфталоцианин, синглетный кислород, флуоресценция, стабильность.

Introduction

Phthalocyanines and their analogues have found applications in various fields, from organic electronics (sensors, solar cells, optical limiters) and catalysis to medicinal chemistry (photodynamic therapy and imaging).[1-6] The problem of the pronounced tendency to aggregation due to the large π-system of macroheterocyclic compounds of this class can be addressed by several different strategies. The first approach involves selecting boron subphthalocyanines as the objects of study. These compounds are cone-shaped, non-planar, and therefore not prone to aggregation.[3] They demonstrate bright fluorescence and high yields of singlet oxygen generation which allows to use them for sensors[7] and visualization,[8,9] as well as photosensitizers for photodynamic therapy of cancer[10-12] and antimicrobial therapy.[13] Another way to address the problem of aggregation is to introduce different sterically hindered substituents.[14,15] Bulky functional groups effectively suppress phthalocyanine aggregation in solutions.[15,16] Aryloxy groups are among the most popular for introduction into phthalocyanine and subphthalocyanine macrocycles.[16-18] Unlike alkyl- and alkoxy-substituted analogs, aryloxy groups are readily introduced *via* nucleophilic substitution reactions.[17] Presence of flexible C-O-C bonds and insertion of some bulky groups directly into phenoxy substituents result in better solubility, higher ability to fluoresce and singlet oxygen generation comparing to unsubstituted analogs. Novakova *et al.* demonstrated that, compared to bulky alkoxy-pyrazinoporphyrazine, 2,6-diisopropylphenoxy substituted pyrazinoporphyrazine exhibited a higher singlet oxygen quantum yield.[19] Makarov *et al.* demonstrated that the introduction of 2,6-dimethylphenoxy leads to the generation of singlet oxygen even in the case of π-extended and aggregation-prone binuclear phthalocyanines.[20] In contrast, alkyl substituted binuclear phthalocyanines are not able to generate singlet oxygen.[21]

In the present study, 2,6-dimethylphenoxy groups were introduced to the periphery of the macrocycle. Compounds with hydrophobic functional groups were chosen for the following reasons. Lipophilic phthalocyanines are more difficult to obtain than their hydrophobic analogs. Due to their greater affinity for the cell membrane, lipophilic complexes penetrate the cell more easily. For the well-known hydrophilic drug *Photosens*, its high degree of hydrophilicity leads to slow absorption by cells and lower photodynamic activity than observed in more hydrophobic analogs - *Holosens* and *Phthalosens*.[22] Moreover, water-soluble phthalocyanines tend to aggregate in water, which reduces their photodynamic activity and, therefore, limits their clinical application. For example, water-soluble silicon phthalocyanine 4 (Pc4), which has undergone clinical trials as a photosensitizer for PDT, was effectively solubilized using Si nanoparticles.[23] Thus, the solubilization procedure is desirable in both cases for hydrophobic and hydrophilic photosensitizers. In addition the main advantage of phthalocyanines and their analogs with lipophilic groups is the possibility to strong hydrophobic binding with human serum albumin[11] and easy transfer to cancer cells. Due to the reasons mentioned above we chose photosensitizers with lipophilic groups and the search of suitable formulation systems for these objects will be the subject of our further investigations.

Boron and magnesium were selected as central ions. The presence of magnesium contributes to an increase in the singlet excited-state lifetime and, consequently, to a higher fluorescence quantum yield. Earlier studies reported phthalocyanine complexes bearing dimethylphenoxy substituents with antimony(V),[15,24] copper(II),[15] silver(I)[25] and phosphorous(V)[26] as the central ion. For the first time, magnesium phthalocyanine and boron subphthalocyanine with such peripheral substituents were obtained.

Experimental

Methods

1,8-Diazabicyclo[5.4.0]undec-7-ene (DBU) (Sigma-Aldrich, 98 %), *N*,*N*-dimethylformamide (DMF) (Sigma-Aldrich, anhydrous, 99.8 %) and BCl_3 (Sigma-Aldrich, 1.0 M in methylene chloride) were used without additional purification. The salts $Zn(OAc)_2{\times}2H_2O$ and $Mg(OAc)_2{\times}4H_2O$ were dried at 70 ^{0}C for 3 h before use. The starting 2,6-dimethylphenoxyphthalonitrile was obtained by analogy with a previously published method.[27] The X-ray data for this nitrile were described by Büyükgüngör *et al.*[28]

The preparation of target compounds was monitored using thin-layer chromatography (TLC). The synthesis of complexes was monitored by both TLC and UV−Vis spectroscopy until the complete disappearance of the starting reagents was observed. TLC was performed using Merck Silica Gel 60 F_{254} neutral flexible plates. Electronic absorption (UV−Vis) spectra were recorded on a JASCO V-770 spectrophotometer using quartz cells (1×1 cm) and the fluorescence spectra were recorded on «Fluorate-02-Panorama» spectrophotometer in a quartz cuvette with an optical path length of 1 cm at room temperature. Matrix assisted laser desorption/ionization time-of-flight (MALDI-TOF) mass spectra were taken on a Bruker Autoflex II mass spectrometer. High-resolution MALDI mass spectra were registered on a Bruker ULTRAFLEX II TOF/TOF instrument.

^{1}H NMR spectra were measured on a Bruker AVANCE 600 spectrometer (600.13 and 100.61 MHz respectively). Chemical shifts are given in ppm relative to $SiMe_4$.

Fluorescence quantum yields of complexes were recorded in DMF using unsubstituted zinc phthalocyanine (Φ_f = 0.17 in DMF[18]) as a standard for phthalocyanine **1** irradiated with the xenon lamp at 610 nm. Rodamine B (Φ_f = 0.42 in DMF[29]) was chosen as a standard for boron subphthalocyanine and irradiated with the xenon lamp at 525 nm. To prevent the internal filter effect, the optical density of sample and standard solutions at the excitation wavelength did not exceed 0.1. Fluorescence quantum yields were determined using a method described in the literature[30] according to the formula:

$$\Phi_f^{\mathrm{X}} = \Phi_f^{st} \frac{F_X(1-10^{-A_{st}})}{F_{st}(1-10^{-A_{\mathrm{X}}})} ,$$

where Φ^{X}_f and Φ^{st}_f are the fluorescence quantum yields of the sample and that of the standard, respectively.

Photochemical properties were studied using a research cell assembled based on a JASCO FLH-740 cuvette holder with installed Arduino board (Leonardo) to control laser.[31] Singlet oxygen quantum yields were determined using the chemical trapping

method. The concentration of dyes (compounds **1** or **2**) in the initial solutions was selected so that their optical density was approximately the same and was C=10^{-6} M. The irradiation wavelength was chosen so that the samples under study had a minimum optical density, while the trap had a maximum absorption. In accordance with this requirement, 1,3-diphenylisobenzofuran (DPBF, Sigma-Aldrich) with a maximum absorption at 415 nm was chosen as a trap. The concentration of DPBF in the solution with photosensitizers was $10 \cdot 10^{-6}$ M.

Unsubstituted zinc phthalocyanine (Φ_Δ = 0.56 in DMF[32]) and Rose Bengal (Φ_Δ = 0.47 in DMF[33]) were chosen as reference compounds for phthalocyanine **1** and subphthalocyanine **2**, respectively.

After adding the DPBF, the cuvette was irradiated with a green laser (λ = 525 nm) for 5 s (compound **2** or Rose Bengal) or a red laser (λ = 650 nm) for 10 s (compound **1** or unsubstituted zinc phthalocyanine). Progress of the reaction between singlet oxygen and DPBF was monitored using UV–Vis spectroscopy. The decrease of absorption band at 415 nm for DPBF was followed upon irradiation with light absorbed by compound used as a standard or by the studied complex.

The decrease in the absorbance of the chemical trap at 415 nm indicated the generation of singlet oxygen by the photosensitizer. The Φ_Δ was measured in the air-saturated solutions, and the following equation was employed for the calculations:[34]

$$\Phi_\Delta^X = \Phi_\Delta^{st} \frac{k_X(1-10^{-A_{st}})}{k_{st}(1-10^{-A_X})},$$

where k_x and k_{st} are the photodegradation rate constants for target photosensitizers and reference compound; A_x and A_{st} are the absorbance at the wavelength of excitation for target photosensitizers and reference. The constants k_x and k_{st} were taken from the slopes in the linear region of the plots obtained for the target complexes and the corresponding slope obtained for the reference compound.

Synthesis

*Magnesium tetra(2,6-dimethylphenoxy) substituted phthalocyanine, **1**.* 2,6-dimethylphenoxyphthalonitrile (150 mg, 0.60 mmol), $Mg(OAc)_2 \cdot 4H_2O$ (81 mg, 0.38 mmol) and DBU (50 μL) were stirred in 1.5 mL of boiling isoamyl alcohol for 5 h (TLC-control: SiO_2, F_{254}, benzene). The reaction mixture was cooled to room temperature, and a MeOH:H_2O (4:1, v/v) mixture added. The precipitate was filtered, washed with a MeOH:H_2O (4:1, v/v) mixture to give compound **1** (82 mg, 54%). UV-Vis (DMF) λ_{max} nm (lg ε): 355 (4.8), 611 (4.5), 679 (5.2). ^{1}H NMR (600.13 MHz, acetone-d_6) δ_H ppm: 2.72–2.75 (s, 6H, H_{CH3}), 7.29–7.42 (m, 3H, H_{Ar}), 7.62 (br, 1H, H_{Pc}), 8.37–8.53 (m, 1H, H_{Pc}), 8.97–9.08 (m, 1H, H_{Pc}). MS (MALDI-TOF) *m/z:* 1005 ($[M]^+$, 100%). MS (MALDI-TOF/TOF) *m/z*: found: 1016.3631 $[M]^+$; molecular formula $C_{64}H_{48}MgN_8O_4$ requires 1016.3648 $[M]^+$.

*Tri(2,6-dimethylphenoxy)substituted subphthalocyanine boron chloride, **2**.* A mixture of 2,6-dimethylphenoxyphthalonitrile (200.0 mg, 0.81 mmol) and boron trichloride (0.8 mL, 1 M solution in CH_2Cl_2) was refluxed in *p*-xylene (6 mL) under argon atmosphere for 1.5 hours. The reaction mixture was cooled to room temperature and diluted with benzene. The insoluble impurities were filtered off, and the resulting solution was concentrated under reduced pressure. The purple precipitate was washed with *n*-hexane and filtered. The resulting precipitate was dried at room temperature to give compound **2** (128 mg, 60%). UV-Vis (DMF) λ_{max} nm (lg ε): 337 (3.7), 515 (3.6), 573 (4.1). ^{1}H NMR (400.13 MHz, $CDCl_3$) δ_H ppm: 2.12 (s, 18H, H_{CH3}), 7.12–7.23 (m, 9H, H_{Ar}), 7.38–8.02 (m, 9H, H_{SubPc}). MS (MALDI-TOF) *m/z*: 755 ($[M\text{-}Cl]^+$, 100%); 790 ($[M]^+$, 40%). IR (diamond) ν cm^{-1}: 710–776 (B-Cl), 1180–1274 (C_{ar}-O-C_{ar}), 1376 (B-N st), 1455–1606 (γ heterocycle), 2851–2919 (CH_3O st). MS (MALDI-TOF/TOF) *m/z*: found: 790.266 $[M]^+$; molecular formula $C_{48}H_{36}BClN_6O_3$ requires 790.263 $[M]^+$.

Results and Discussion

To obtain the target 2,6-dimethylphenoxy-substituted compounds **1** and **2**, a classical template synthesis procedure was used. The starting 2,6-dimethylphenoxyphthalonitrile was refluxed in a high-boiling solvent in the presence of a template ion source. Phthalocyanine metal complex was carried out in boiling isoamyl alcohol in the presence of 1,8-diazabicyclo (5.4.0)undec-7-ene (DBU) as a base. The corresponding metal acetate salt was used as metal sources. A similar approach was previously used to synthesize 2,6-dimethylphenoxy substituted copper phthalocyanine[24] (Scheme 1).

The synthesis of subphthalocyanines was conducted in a boiling *p*-xylene using the excess of boron trichloride as a source of boron ion. The target complexes **1** and **2** were obtained in moderate yields. It should be noted that the target compounds were obtained as a mixture of inseparable regioisomers (four isomers for compound **1** and two isomers for compound **2**).

Target phthalocyanine complexes were identified using high-resolution mass spectrometry, NMR and IR spectroscopy. Mass spectra of magnesium and boron complexes showed intense molecular ion peaks. The experimentally observed isotope patterns for peaks of molecular ions $[M]^+$ are in good agreement with theoretically calculated ones (Figure 1). In addition for axially-substituted subphthalocyanine **2** the typical cleavage of axial chlorine was observed under the laser ionisation.

In the UV-Vis spectra of target compounds, the most intense *Q* bands were observed in visible region, which corresponds to the electron transfer between the HOMO and LUMO. As is typical for macroheterocycles of this class, the *Q* band position of subphthalocyanine **2** is about 100 nm hypsochromically shifted compared to phthalocyanine **1** (574 nm and 683 nm for complexes **2** and **1** respectively) (Figure 2). Presence of regioisomers resulted in insignificant splitting of *Q* band of compound **1**(Figure 2).

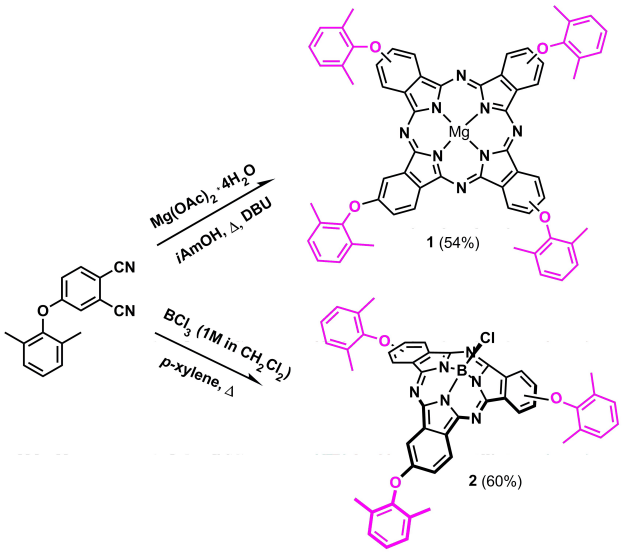

Scheme 1. Synthesis of compounds **1** and **2**.

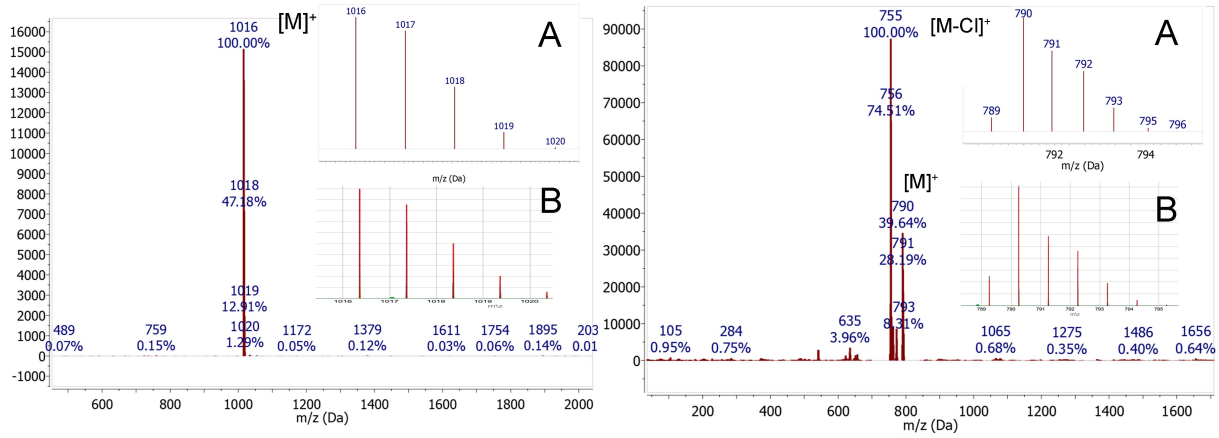

Figure 1. MALDI TOF mass spectra (positive ion mode) of complexes **1** (left) and **2** (right). The inserts show the experimentally obtained (A) and theoretically calculated (B) isotopic patterns for molecular ions $[M]^+$.

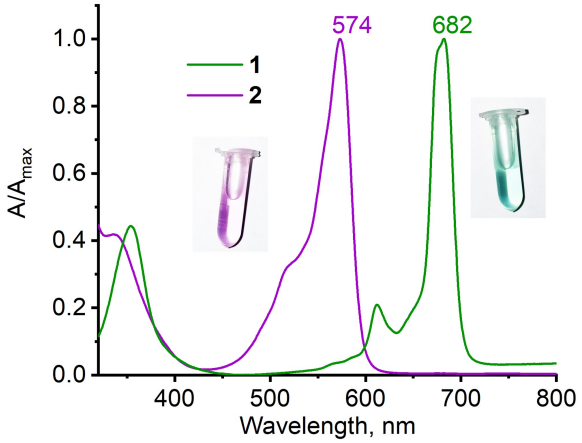

Figure 2. UV-Vis spectra of compounds **1** (green line) and **2** (purple line) in DMF.

Based on the data of Table 1, some features of the UV-Vis spectroscopy of aryloxy substituted phthalocyanines and subphthalocyanines can be noted. As noted previously with respect to other phthalocyanines[35] introduction of aryloxy groups into the alpha positions of the macroheterocycle leads to a greater bathochromic shift of the *Q*-band compared to beta-substituted phthalocyanines ($^{3\text{-MeOPhOEtO}}$PcZn *vs.* $^{4\text{-MeOPhOEtO}}$PcZn, Table 1). The presence of aryloxy fragment in β-positions of phthalocyanine results in about 10 nm bathochromic shift of the *Q* band (10 nm) for phthalocyanine **1** comparing to unsubstituted magnesium phthalocyanine (PcMg, see Table 1). The introduction of additional substituents into *para*-positions of phenoxy groups doesn't influence on the *Q* band position (^{PhO}SubPcBCl *vs.* ^{CO2EtC6H4O}SubPcBCl, Table 1). A small bathochromic shift was observed by Makhseed *et al.*[36] when going from chlorine to bromine atoms at the 2,6 positions of the phenoxy groups (^{ClC6H4O}PcMg *vs.* ^{BrC6H4O}PcMg, Table 1).

The stability of the complexes **1** and **2** was investigated in different organic solvent: toluene, $CHCl_3$, DMF, THF (Figures 3 and 4). The best results were obtained using THF and DMF. Therefore, DMF was chosen as a less volatile solvent for measuring fluorescence and singlet oxygen quantum yields.

The calculated molar absorption coefficient for the phthalocyanine complex in DMF was lgε = 5.2, confirming a decrease in aggregation and an improvement in solubility. The concentration at which deviation from the Bouguer-Lambert-Baer law begins was not detected; it probably corresponds to a concentration outside the detection range of our spectrophotometer.

The absorption and emission spectra of target compounds are mirror images of each other (Figure 5). The Stokes shift of the *Q* bands is 9 nm (compound **1**) and 11 nm (compound **2**) which is typical for phthalocyanines and their analogs. The fluorescence quantum yields of compounds **1** and **2** were measured in DMF using unsubstituted zinc phthalocyanine as the standard (Φ_{fl} = 0.17 in DMF[37]) for phthalocyanine **1** and Rhodamine B for subphthalocyanine **2**. Subphthalocyanine **2** was shown to exhibit approximately twice the fluorescence intensity of phthalocyanine **1** (Table 1). Furthermore, the introduction of methyl groups into the 2,6 positions of the phenoxy substituents leads to an increase in Φ_{fl} when going from ^{PhO}SubPcBCl to compound **2**. In the case of introduction of methoxy groups ($^{2,6\text{-MeOPhO}}$PcMg[38]) the Φ_{fl} value was similar to compound **1**. Literature data shows that introduction of more flexible substituents especially in alpha position of phthalocyanine macrocycle resulted in drop in fluorescence quantum yield (Table 1, $^{4\text{-MeOPhOEtO}}$PcZn and $^{3\text{-MeOPhOEtO}}$PcZn). The high values of fluorescence quantum yields were observed for subphthalocyanine ^{CO2EtC6H4O}SubPcBCl and magnesium phthalocyanines ^{ClC6H4O}PcMg and ^{BrC6H4O}PcMg. Makhseed *et al.*[36] demonstrated that replacing the central ion from Mg(II) to Zn(II) resulted in a decrease in the fluorescence quantum yield and an increase in the singlet oxygen quantum yield.

The singlet oxygen quantum yield (Φ_Δ^{st}) for complexes **1**, **2** was determined using the chemical trapping method.[40] This method is based on a decrease in the absorption intensity of a chemical trap, 1,3-diphenylisobenzofuran (DPBP), at 415 nm when irradiated in the presence of photosensitizers (Figure 6A,C). Spectral changes are caused by the destruction of the isobenzofuran aromatic system.

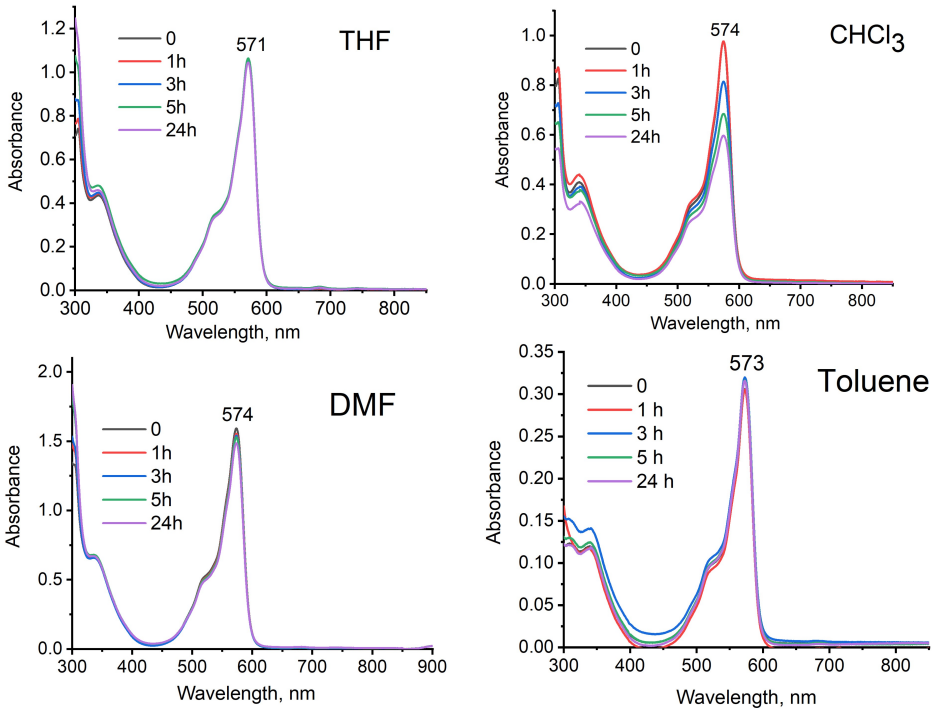

Figure 3. Stability of subphthalocyanine **2** in different solvents measured by UV-Vis spectroscopy (aerobic conditions, complete darkness, $C = 1.2 \cdot 10^{-4}$ M, half-life time in $CHCl_3$ was about 24 h).

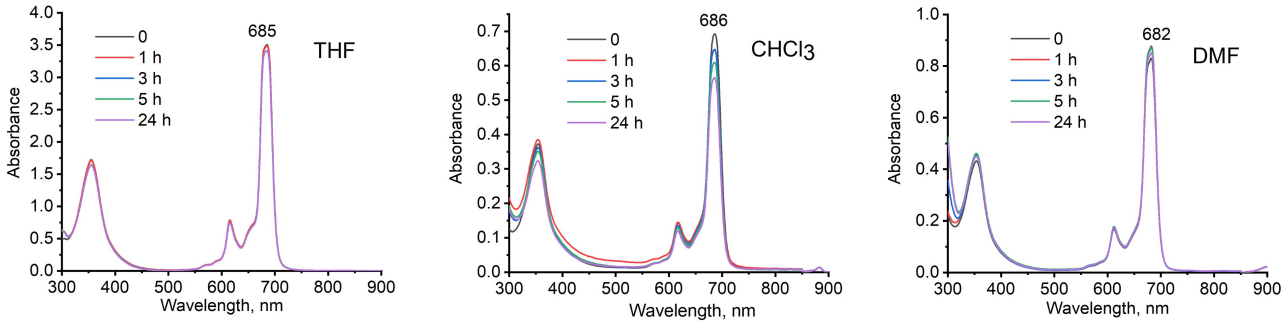

Figure 4. Stability of phthalocyanine **1** in different solvents measured by UV-Vis spectroscopy (aerobic conditions, complete darkness, $C = 6 \cdot 10^{-6}$ M, half-life time in $CHCl_3$ was > 24 h).

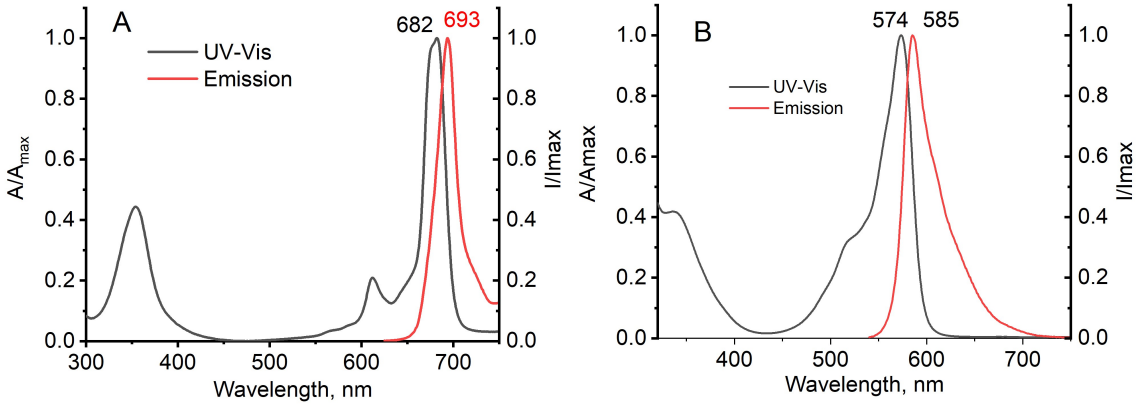

Figure 5. UV-Vis (black line) and emission (red line) spectra of substituted phthalocyanine (A) and subphthalocyanine (B) in DMF. In the case of emission spectra λ_{ex} = 610 nm for magnesium phthalocyanine **1** and λ_{ex} = 525 nm for subphthalocyanine **2**.

Table 1. Photophysical data for compounds **1** and **2** and literature data for other aryloxy substituted complexes.

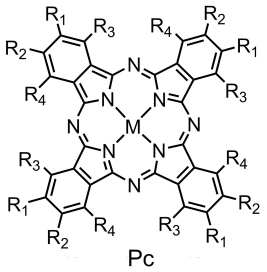

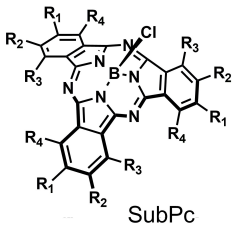

Compound	Type	R_1	R_2	R_3	R_4	M	λ_{abs}, nm	λ_{em}, nm	Φ_{fl}	Φ_{Δ}	Solvent
1	Pc	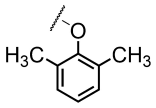	H	H	H	Mg	682	693	0.23	0.42	DMF
2	SubPc	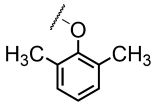	H	H	H	BCl	574	585	0.43	0.27	DMF
$^{4\text{-MeOPhOEtO}}$PcZn [39]	Pc	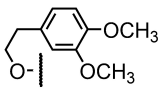	H	H	H	Zn	683	698	0.15	0.61	DMSO
$^{3\text{-MeOPhOEtO}}$PcZn [39]	Pc	H	H	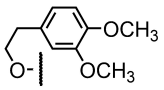	H	Zn	706	720	0.08	0.49	DMSO
$^{2,6\text{-MePhO}}$PcH$_2$ [20]	Pc	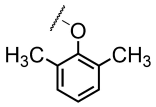	=R_1	H	H	HH	701 and 664	706	0.33	0.10	toluene
$^{2,6\text{-MeOPhO}}$PcMg [38]	Pc	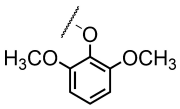	H	H	H	Mg	675	690	0.27	Not meas-ured	DMF
^{ClC6H4O}PcMg [36]	Pc	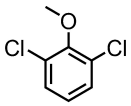	=R_1	H	H	Mg	672	676	0.62	0.21	THF
^{ClC6H4O}PcZn [36]	Pc	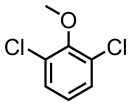	=R_1	H	H	Zn	671	675	0.33	0.53	THF
^{BrC6H4O}PcMg [36]	Pc	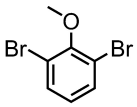	=R_1	H	H	Mg	675	679	0.50	0.24	THF
^{BrC6H4O}PcZn [36]	Pc	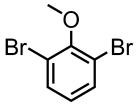	=R_1	H	H	Zn	673	676	0.32	0.53	THF

Table 1. Continuation.

PcMg[27]	Pc	H	H	H	H	Mg	669	681	0.23	0.28	DMF
^{PhO}SubPcBCl[11]	SubPc	OC_6H_5	$=R_1$	H	H	BCl	572[a]	582[a]	0.13[a]	0.48[b]	*n*-propanol
^{CO2EtC6H4O}SubPcBCl[11]	SubPc	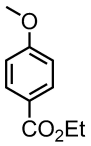	$=R_1$	H	H	BCl	569[a]	582[a]	0.50[a]	0.47[b]	*n*-propanol

[a] – measured in *n*-propanol
[b] – measured in toluene

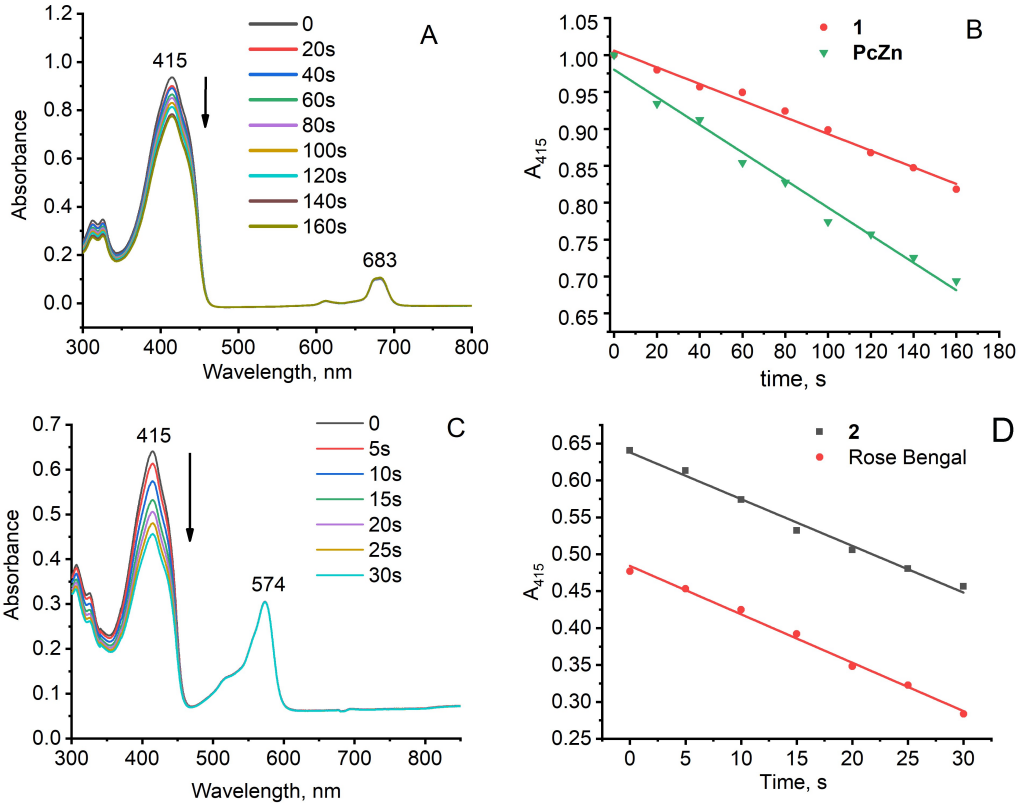

Figure 6. Changes in the UV-Vis spectra of DMF solution of DPBF (C=10·10^{-6} M) in the presence of magnesium phthalocyanine **1** (A, B) or boron subphthalocyanine **2** (C, D) during the irradiation (for photosensitizers C=10^{-6} M). The decrease in DPBF absorption is shown by arrows.

Unsubstituted zinc phthalocyanine (Φ_Δ^{st} = 0.56 in DMF[32]) served as the reference compound in the case of phthalocyanine **1** due to the similarity of the absorption region. Rose Bengal was used as a reference compound for substituted boron subphthalocyanine: Φ_Δ^{st} = 0.47 in DMF.[33]

The photodegradation reaction of the highly reactive chemical trap DPBF is zero-order.[40] Photodegradation rate constants were determined as the slopes of the linear graphs of DPBF degradation (Figure 6B,D). The degradation rate constants of DPBF and the corresponding R^2 values were:

k= 9·10^{-4} M·s^{-1} and R^2 = 0.99 for phthalocyanine **1**;
k= 1.8·10^{-3} M·s^{-1} and R^2 = 0.99 for ZnPc;
k= 6.3·10^{-3} M·s^{-1} and R^2 = 0.99 for subphthalocyanine **2**;
k= 6.8·10^{-3} M·s^{-1} and R^2 = 0.99 for Rose Bengal.

For phthalocyanine **1**, an increase in the quantum yield of singlet oxygen is observed compared to subphthalocyanine **2**, which is a result of competition between the processes of fluorescence and the generation of singlet oxygen. It is interesting that, despite the presence of heavy bromine atoms at the 2,6 positions of the phenoxy group, Φ_Δ of the corresponding compound ^{BrC6H4O}PcMg is low (Table 1). At the same time, the values of Φ_Δ increase significantly when moving from the central Mg ion to the central Zn ion (*e.g.* ^{BrC6H4O}PcMg *vs.* ^{BrC6H4O}PcZn).[36] It is noteworthy that the quantum yield of singlet oxygen of the obtained phthalocyanine complex is higher than that of *Photosens*, a drug approved for photodynamic therapy (Φ_Δ = 0.19[41] in DMF).

Conclusions

New magnesium phthalocyanine and boron subphthalocyanine bearing bulky 2,6-dimethylphenoxy peripheral groups were obtained. Due to the bulky functional groups, the target complexes exhibit high solubility and stability in THF and DMF. 2,6-Dimethylphenoxy substituted subphthalocyanine demonstrates high value of fluorescence quantum yield up to Φ_{fl} = 0.43. In contrast, the phthalocyanine compound exhibits a better singlet oxygen quantum yield (Φ_{Δ} = 0.42) compared with the target subphthalocyanine. It is noteworthy that for the 2,6-dimethylphenoxy substituted phthalocyanine magnesium complex the Φ_{Δ} value is higher than the corresponding value for *Photosens*, a drug approved for photodynamic therapy. Due to the ability to absorb light and fluoresce in the transparency range of biological tissues (600–900 nm) and high efficiency of singlet oxygen generation, the magnesium complex is a more promising compound for photodynamic therapy.

Acknowledgements. Synthesis, identification, optical and photochemical properties of magnesium phthalocyanine was supported by the Russian Science Foundation Grant No 24-73-00062. Synthesis and photochemical properties of boron subphthalocyanine was supported by the Russian Science Foundation Grant No 23-73-10076.

Author Contribution. E.A. Gorbunova: conceptualization, writing – review and editing, funding acquisition; K.A. Kisliak: validation, investigation, writing – original draft; A.S. Agranat: investigation, writing – original draft, visualization; V.L. Baklagin: investigation, writing – review and editing; V.V. Bukhalin: investigation; I.G. Abramov: writing – review and editing; and T.V. Dubinina: writing – review and editing, supervision, funding acquisition.

References

1. Znoyko S.A., Maizlish V.E., Koifman O.I. *ChemChemTech* **2024**, *67*, 7–35.
2. Labella J., Torres T. *Trends in Chemistry* **2023**, *5*, 353–366.
3. Lavarda G., Labella J., Martínez-Díaz M.V., Rodríguez-Morgade M.S., Osuka A., Torres T. *Chem. Soc. Rev.* **2022**, *51*, 9482–9619.
4. Danilova E.A., Galanin N.E., Islyaikin M.K., Maizlish V.E., Berezina G.R., et al. *ChemChemTech* **2023**, *66*, 111–119.
5. Ömeroğlu İ., Göksel M., Kussovski V., Mantareva V., Durmuş M. *Macroheterocycles* **2019**, *12*, 255–263.
6. Salazar A., Labella J., Kumar S., Torres T., de la Torre G. *Adv. Synth. Catal.* **2024**, *366*, 934–941.
7. Alfred M.A., Lang K., Kirakci K., Stuzhin P., Zimcik P., Labuta J., Novakova V. *Dalton Trans.* **2024**, *53*, 2635–2644.
8. Yurt F., Ince M., Er O., Melis Soylu H., Ocakoglu K., Yilmaz O. *Photodiagn. Photodyn. Ther.* **2019**, *26*, 361–365.
9. van de Winckel E., Mascaraque M., Zamarrón A., de la Fuente Á.J., Torres T., de la Escosura A. *Adv. Funct. Mater.* **2018**, *28*, 1705938.
10. Demuth J., Gallego L., Kozlikova M., Machacek M., Kucera R., Torres T., Martinez-Diaz M.V., Novakova V. *J. Med. Chem.* **2021**, *64*, 17436–17447.
11. Burtsev I.D., Dubinina T.V., Egorov A.E., Kostyukov A.A., Shibaeva A.V., et al. *Dyes Pigm.* **2022**, *207*, 110690.
12. Casellas N.M., Dai G., Xue E.Y., Fonseca A., Ng D.K.P., García-Iglesias M., Torres T. *Chem. Commun.* **2022**, *58*, 669–672.
13. Dharmaratne P., Sapugahawatte D.N., Wang B., Chan C.L., Lau K.-M., et al. *Eur. J. Med. Chem.* **2020**, *200*, 112341.
14. Cyza M., Gut A., Łapok Ł., Solarski J., Knyukshto V., Kępczyński M., Nowakowska M. *J. Photochem. Photobiol. A: Chem.* **2018**, *358*, 265–273.
15. Isago H., Fujita H., Sugimori T. *J. Inorg. Biochem.* **2012**, *117*, 111–117.
16. Makhseed S., Samuel J. *Dyes Pigm.* **2009**, *82*, 1–5.
17. Baklagin V.L., Bukhalin V.V., Abramov I.G. *Macroheterocycles* **2025**, *18*, 170–194.
18. Abramov I.G., Baklagin V.L., Bukhalin V.V., Maizlish V.E., Rassolova A.E. *From Chemistry to Technology: Step by Step [От химии к технологии шаг за шагом]* **2022**, *3*(4), 53–60.
19. Novakova V., Zimcik P., Miletin M., Vůjtěch P., Franzová Š. *Dyes Pigm.* **2010**, *87*, 173–179.
20. Makarov S., Litwinski C., Ermilov E. A., Suvorova O., Röder B., Wöhrle D. *Chem. Eur. J.* **2006**, *12*, 1468–1474.
21. Mack J., Liang X., Dubinina T.V., Tomilova L.G., Nyokong T., Kobayashi N. *J. Porphyrins Phthalocyanines* **2013**, *17*, 489–500.
22. Brilkina A.A., Dubasova L.V., Sergeeva E.A., Pospelov A.J., Shilyagina N.Y., Shakhova N.M., Balalaeva I.V. *J. Photochem. Photobiol. B: Biol.* **2019**, *191*, 128–134.
23. Zhao B., Yin J.–J., Bilski P.J., Chignell C.F., Roberts J.E., He Y.-Y. *Toxicol. Appl. Pharmacol.* **2009**, *241*, 163–172.
24. Isago H., Kagaya Y., Fujita H., Sugimori T. *Dyes Pigm.* **2011**, *88*, 187–194.
25. Isago H., Fujita H., Nakai S., Sugimori T. *J. Inorg. Biochem.* **2021**, *219*, 111427.
26. Isago H., Fujita H., M Hirota., Sugimori T., Kagaya Y. *J. Porphyrins Phthalocyanines* **2013**, *17*, 763–771.
27. Kudo T., Kimura M., Hanabusa K., Shirai H., Sakaguchi T. *J. Porphyrins Phthalocyanines* **1999**, *03*, 65–69.
28. Büyükgüngör O., Koşar B., Akdemir N., Ağar E., Gümrükçüoğlu I. *Acta Crystallogr. Sect. E* **2005**, *E61*, o335–o336.
29. Zhang X.-F., Zhang Y., Liu L. *J. Luminesc.* **2014**, *145*, 448–453.
30. Brouwer A.M. *Pure Appl. Chem.* **2011**, *83*, 2213–2228.
31. Gorbunova E.A., Stepanova D.A., Kosov A.D., Bolshakova A.V., Filatova N.V., et al. *J. Photochem. Photobiol. A: Chem.* **2022**, *426*, 113747.
32. Ogunsipe A., Durmuş M., Atilla D., Gürek A.G., Ahsen V., Nyokong T. *Synth. Met.* **2008**, *158*, 839–847.
33. Redmond R.W., Gamlin J.N. *Photochem. Photobiol.* **1999**, *70*, 391–475.
34. Lutkus L.V., Rickenbach S.S., McCormick T.M. *J. Photochem. Photobiol. A: Chem.* **2019**, *378*, 131–135.
35. Kobayashi N., Ogata H., Nonaka N., Luk'yanets E.A. *Chem. Eur. J.* **2003**, *9*, 5123–5134.
36. Makhseed S., Ghazal B., Abdelmoniem A.M., Novakova V., Zimcik P. *RSC Adv.* **2015**, *5*, 58854–58864.
37. Ogunsipe A., Maree D., Nyokong T. *J. Mol. Struct.* **2003**, *650*, 131–140.
38. Pişkin M., Öztürk Ö.F., Odabas Z. *MANAS J. Eng.* **2021**, *9*, 58–64.
39. Güzel E., Günsel A., Tüzün B., Atmaca G.Y., Bilgiçli A.T., Erdoğmuş A., Yarasir M.N. *Polyhedron* **2019**, *158*, 316–324.
40. Bresolí-Obach R., Torra J., Zanocco R.P., Zanocco A.L., Nonell S. In: *Reactive Oxygen Species: Methods and Protocols* (Espada J., Ed.) Springer US, New York, **2021**. pp. 165–188.
41. Makarov S.G., Schnurpfeil G., Rychagova E.A., Ketkov S.Y., Suvorova O.N., Wöhrle D. *J. Porphyrins Phthalocyanines* **2017**, *21*, 844–849.

Received 12.04.2026
Accepted 30.04.2026